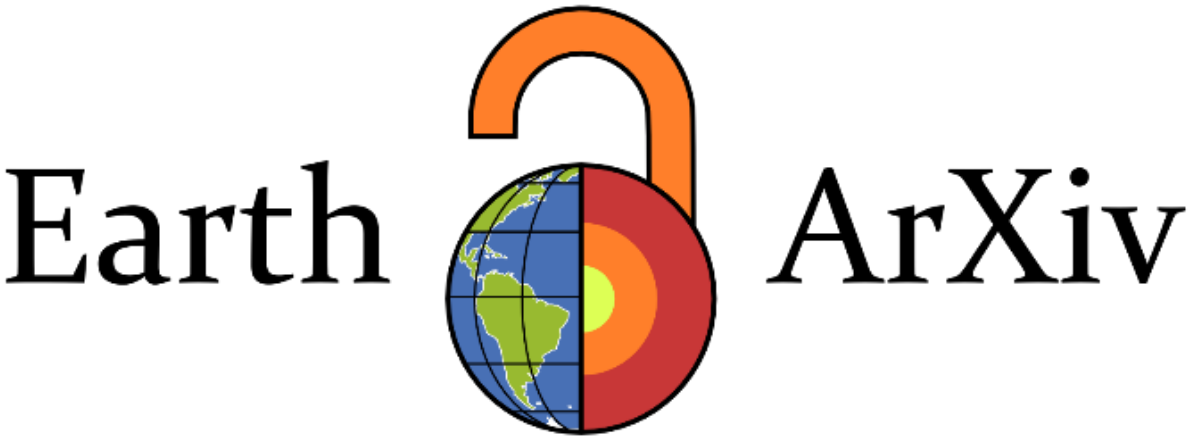

# A Multi-Dimensional Framework for Diagnosing Inconsistencies in Remote Sensing-Based Ecosystem Assessment

Oluwafemi David Bejide, University of Ibadan, Nigeria

Email: Bejidedavid37@gmail.com

Corresponding Author

Oluwafemi David Bejide

Email: Bejidedavid37@gmail.com

Abstract:

Remote sensing-based ecosystem assessment increasingly relies on the integration of spectral, structural, and model-derived datasets; however, inconsistencies among these data sources can produce divergent representations of vegetation dynamics and carbon processes. This study proposes a multi-dimensional framework to diagnose such inconsistencies by integrating scale, dimensional, and variable components within a unified analytical structure. Using Ekiti State, Nigeria as a heterogeneous tropical test landscape, scale inconsistency was assessed through comparison of CASA-derived and MODIS Net Primary Productivity (NPP), dimensional inconsistency through threshold-based validation of land use/land cover (LULC) against GEDI-derived canopy height (≥5 m and ≥10 m), and variable inconsistency through non-proportional changes between aboveground biomass (AGB) and canopy height model (CHM).

Results indicate persistent scale-related discrepancies, with CASA systematically overestimating NPP relative to MODIS and exhibiting weak spatial correspondence ($R^2 \approx 0.03$ in 2020 and 0.04 in 2025). Dimensional inconsistency was substantial (mean ≈ 0.41), reflecting systematic mismatch between spectral and structural representations of forest extent. In contrast, variable inconsistency was relatively low (mean VI = 0.18), indicating broadly proportional structural–carbon responses across most of the landscape, with localized divergence in disturbed and non-vegetated areas. Integration of these components yielded a Multi-Dimensional Inconsistency Index (MDII) of 0.26, indicating moderate overall inconsistency dominated by dimensional mismatch.

These findings demonstrate that inconsistencies in remote sensing-based ecosystem assessment are systematic and multi-faceted, arising from differences in spatial scale, data representation, and model structure, and highlight the importance of integrated frameworks for improving the reliability of ecosystem monitoring in complex landscapes.

**Keywords:** Net Primary Productivity (NPP), Aboveground biomass (AGB), Canopy height model (CHM), Spectral–structural mismatch, CASA–MODIS comparison.

## Introduction

The accurate estimation of ecosystem services is critical for environmental decision-making, as governments and policymakers increasingly rely on such information to guide climate mitigation strategies, land-use planning, and sustainable development initiatives (Costanza et al., 2014; IPCC,

2021). Remote sensing has become a cornerstone of ecosystem monitoring, providing spatially continuous and temporally consistent observations of vegetation dynamics, forest extent, and carbon fluxes at regional to global scales (Turner et al., 2003; Pettorelli et al., 2014). Advances in satellite technologies have enabled the integration of spectral, structural, and model-based datasets, including optical imagery, spaceborne LiDAR, and productivity models, to quantify ecosystem condition and function (Running et al., 2004; Dubayah et al., 2020).

Despite these advances, important limitations persist in the use of remote sensing for ecosystem assessment. These include generalization effects associated with coarse spatial resolution, scale mismatches between global products and local conditions, and temporal inconsistencies across datasets (Atkinson & Tate, 2000; Woodcock & Strahler, 1987). As a result, different datasets derived from varying sensors, resolutions, and modelling approaches may produce divergent representations of ecosystem dynamics, leading to uncertainty in the interpretation of vegetation trends and carbon processes (Saatchi et al., 2011; Mitchard et al., 2013).

One major source of inconsistency arises from the mismatch between two-dimensional spectral classifications and three-dimensional structural representations of vegetation, often resulting in divergence between spectrally defined and structurally defined forest conditions (Bejide et al., 2026; Dubayah et al., 2020). Land cover maps derived from optical remote sensing typically rely on discrete categorical classes represented as homogeneous spatial units, which often fail to capture the internal heterogeneity of ecosystems, particularly in landscapes undergoing rapid anthropogenic change (Hansen et al., 2013; Herold et al., 2008). Consequently, significant disagreement can occur between spectral-based forest classifications and structural metrics such as canopy height, especially when evaluated across different height thresholds in heterogeneous environments (Dubayah et al., 2020).

Similarly, scale-dependent inconsistencies have been widely observed between coarse-resolution global products and locally calibrated models. Discrepancies between CASA-based estimates and MODIS-derived productivity illustrate how spatial resolution and modelling assumptions influence the representation of carbon dynamics (Running et al., 2004; Zhao & Running, 2010; Bejide & Olaniran, 2026). These inconsistencies highlight the challenges of applying generalized global datasets to locally complex landscapes.

In addition, increasing evidence points to spectral–structural decoupling in forested ecosystems, where aboveground biomass declines without corresponding changes in spectral classification (Bejide et al., 2026). In such cases, forests may remain classified as intact in land-cover maps while undergoing structural thinning due to selective logging, fuelwood extraction, or other disturbance processes, Gao et al. (2019). This phenomenon reflects the broader challenge of detecting forest degradation using conventional remote sensing approaches. While deforestation can be readily identified through categorical land-cover change, degradation involves subtle alterations in forest structure, composition, and function that are more difficult to capture (Mbow et al., 2015). As highlighted by Gao et al. (2019), the complexity of degradation processes, combined with limitations in spatial and temporal resolution, makes it difficult to quantify biomass loss and accurately represent ecosystem change using remote sensing alone. Similar patterns of structural–carbon divergence have been observed in recent studies integrating LiDAR and multi-sensor data, where reductions in biomass occur without proportional changes in canopy height or spectral signals (Bejide et al., 2026).

These limitations underscore a broader challenge in ecosystem monitoring: remote sensing products often provide incomplete or inconsistent representations of ecosystem state when considered in isolation. While previous studies have examined individual sources of uncertainty—such as scale effects, classification errors, or modelling assumptions—there remains a lack of a unified analytical framework that systematically integrates these inconsistencies across spectral, structural, and carbon dimensions within a single assessment.

This study addresses this gap by proposing a unified framework for diagnosing spectral–structural–carbon inconsistencies in remote sensing-based ecosystem assessment. Using a heterogeneous tropical landscape as a testbed, the study integrates scale-dependent comparisons between productivity datasets, structural–carbon relationships derived from LiDAR and biomass estimates, and threshold-based validation of spectral land-cover classifications. By combining these dimensions within a consistent analytical structure, the framework provides a systematic approach for identifying, quantifying, and interpreting divergence across commonly used Earth observation products. The proposed approach contributes to improving the reliability of remote sensing-based ecosystem monitoring and offers insights for more accurate interpretation of vegetation dynamics and carbon processes in complex landscapes.

This study aims to develop a unified framework for diagnosing inconsistencies in remote sensing-based ecosystem assessment by integrating scale, dimensional, and variable components. Specifically, the study quantifies scale inconsistency in net primary productivity by comparing CASA-derived and MODIS estimates across two temporal periods, evaluates dimensional inconsistency between spectral land-cover classifications and canopy structure using FAO-aligned height thresholds (≥5 m and ≥10 m), and assesses variable inconsistency between canopy height and aboveground biomass to examine structural–carbon decoupling under disturbance. These components are subsequently integrated into a composite Multi-Dimensional Inconsistency Index (MDII) to identify areas of compounded ecosystem representation uncertainty.

## Methodology

### Study area

Ekiti State is located in southwestern Nigeria (7°15′–8°05′N, 4°45′–5°45′E), bounded by Kwara, Kogi, Osun, and Ondo States. The region lies within a rainforest–savanna transition zone, with dense rainforest in the south and Guinea savanna in the north. It experiences a tropical climate with mean temperatures of 27–32°C and annual rainfall of ~1,238 mm, following a bimodal pattern with an August break. Despite its ecological significance, the area has undergone substantial forest degradation driven by population growth, urban expansion, and timber extraction, resulting in biodiversity loss and increasing vulnerability to vegetation transition toward savanna conditions (Festus, 2012).

### Multi-dimensional inconsistency framework

This study proposes a multi-dimensional framework for diagnosing inconsistencies in remote sensing-based ecosystem assessment. The framework integrates three components: scale inconsistency, variable inconsistency, and dimensional inconsistency.

Scale inconsistency (SI) represents the disagreement between productivity estimates derived from datasets with different spatial resolutions, quantified here as the difference between CASA-derived and MODIS NPP. Variable inconsistency (VI) captures the divergence between structurally related variables, specifically canopy height and aboveground biomass (AGB), and reflects structural–carbon decoupling under disturbance. Dimensional inconsistency ($DI_2$) describes the mismatch

between two-dimensional spectral land-cover classifications and three-dimensional canopy structure, assessed using threshold-based comparisons between LULC and canopy height.

To enable integrated assessment, these components are normalized and combined into a composite Multi-Dimensional Inconsistency Index (MDII), which identifies areas where multiple inconsistencies co-occur. The framework is applied to two temporal reference years to evaluate the persistence and evolution of ecosystem representation discrepancies.

**Data Sources:**

The study used multi-sensor remote sensing images from Landsat 8 (OLI, 30m), Sentinel 1 & 2 (10m), ALOS PALSAR (25m), Shuttle Radar Thematic Mapper (SRTM, 30m), MODIS/061/MOD17A3HG (500m), ERA5-Land Climate, and Global Ecosystem Dynamics Investigation (25m) etc. To maintain methodological consistency across temporal analyses, the same input datasets, predictor variables, preprocessing steps, and modelling configurations were applied to both 2020 and 2025. Sampling procedures, feature engineering, and model parameters were held constant, ensuring that interannual differences in results are attributable to data variation rather than differences in analytical workflow.

**Scale Inconsistency Between Carnegie Ames Standard Approach (CASA) and MODIS Net Primary Productivity.**

Scale inconsistency was evaluated by comparing the MODIS Net Primary Productivity (NPP) dataset (500 m) with the Carnegie–Ames–Stanford Approach (CASA) model, initially developed at 30 m resolution. The CASA model is a light use efficiency (LUE) model expressed using equation 1

$$NPP = PAR \times fPAR \times LUE_{max} \times T_{stress} \times Water_{stress} \quad (1)$$

Where PAR = Photosynthetic Active Radiation, fPAR = fraction of Photosynthetic Absorbed Radiation, LUE = Light use efficiency (0.55), T = Temperature stress, and W = Water stress

Water stress was estimated using the Thornthwaite formulation (Equation 2)

$$Water_{stress} = 0.5 + \left(0.5 \times \frac{AET}{PET}\right) \quad (2)$$

The fraction of absorbed PAR was derived from NDVI as in equation 3

$$fPAR = \left(\frac{NDVI - NDVI_{min}}{NDVI_{max} - NDVI_{min}}\right) \times 0.95 \quad (3)$$

The CASA-derived NPP was aggregated to 500 m resolution to enable direct comparison with the MODIS product. To ensure methodological consistency, identical processing procedures were applied to both datasets. Scale inconsistency was computed using equation 4.

$$Scale\ inconsistency\ (SI) = \left(\frac{CASA_{NPP} - MODIS_{NPP}}{\max(CASA_{NPP}, MODIS_{NPP}}\right) \quad (4)$$

The equation was applied for 2020, and 2025, while the mean Scale inconsistency was calculated.

**Dimensional Inconsistency Index (DI) using FAO 5m and 10m threshold.**

Dimensional inconsistency was assessed by comparing two-dimensional (2D) spectral forest classification derived from Land Use/Land Cover (LULC) with three-dimensional (3D) structural forest representation derived from GEDI LiDAR canopy height data.

LULC classification was produced using a fusion of ALOS PALSAR, Landsat spectral bands, and vegetation indices (NDVI, NDMI, and NIRv). Topographic variables derived from SRTM, including elevation and slope, were incorporated to improve discrimination of built-up areas, open surfaces, and rocky outcrops. Supervised classification was conducted using Random Forest and Support Vector Machine algorithms to classify the landscape into water, barren land, built-up areas, cultivated land, shrublands, and forest.

The LULC output was subsequently reclassified into binary forest (1) and non-forest (0), representing a 2D spectral definition of forest.

The GEDI-derived canopy height model (CHM) was used to represent forest structure and was reclassified into binary forest/non-forest using the Food and Agriculture Organization (FAO) conceptual forest definition based on height thresholds of ≥5 m and ≥10 m. The Dimension inconsistency was calculated using (Equation 5).

$$Dimension\ Inconsistency = (LULC_{Forest} - CHM_{Forest}) \quad (5)$$

**Variable Inconsistency between Aboveground Biomass and Canopy Height Index.**

Aboveground biomass (AGB) and canopy height models (CHM) were generated independently using GEDI Level 4A and Level 2A datasets, respectively. A total of thirty-eight predictor

variables were used, including spectral indicators (NDVI, NDMI, SWIR bands), structural metrics (SAR-derived indices and backscatter from Sentinel-1 and ALOS PALSAR), soil properties (SOC, bulk density, pH), topographic variables (slope and elevation), and climatic variables (vapour pressure deficit, actual evapotranspiration, and potential evapotranspiration).

Random Forest was employed for model development and prediction within the Google Earth Engine environment. AGB and CHM were modelled independently to avoid circularity and ensure unbiased comparison. Relative changes were computed as:

$$AGB_{change} = \frac{AGB_{2025} - AGB_{2020}}{AGB_{2020}} \quad (6)$$

$$CHM_{change} = \frac{CHM_{2025} - CHM_{2020}}{CHM_{2020}} \quad (7)$$

Variable inconsistency was then defined as:

$$Variable\ Inconsistency = (AGB_{change} - CHM_{change}) \quad (8)$$

**Multi-Dimensional Inconsistency Index (MDII)**

To integrate the different sources of inconsistency, a Multi-Dimensional Inconsistency Index (MDII) was developed by combining scale inconsistency (SI), dimensional inconsistency (DI), and variable inconsistency (VI).

The SI values for 2020 and 2025 were averaged to obtain a single scale inconsistency layer:

$$SI_{mean} = \frac{SI_{2025} + SI_{2020}}{2} \quad (9)$$

Similarly, dimensional inconsistency was computed across both thresholds (5 m and 10 m) and years (2020 and 2025), and averaged as:

$$DI_{mean} = \frac{DI_{2020,5m} + DI_{2020,10m} + DI_{2025,5m} + DI_{2025,10m}}{4} \quad (10)$$

Variable inconsistency was derived as a change-based measure across the 2020–2025 period and therefore represented a single layer. The Multi-Dimensional Inconsistency Index was then calculated as the arithmetic mean of the three components:

$$MDII = \frac{SI_{mean} + DI_{mean} + VI}{3} \quad (11)$$

The MDII provides a spatially explicit representation of the degree to which different remote sensing-derived indicators of ecosystem condition diverge. Values close to 0 indicate strong agreement across dimensions, while higher values indicate increasing levels of inconsistency.

For interpretation, MDII values were classified into three categories: low inconsistency (<0.20), moderate inconsistency (0.20–0.40), and high inconsistency (>0.40).

## Results

### Scale Inconsistency Between CASA and MODIS NPP

After aggregation of CASA-derived NPP to 500 m to ensure scale consistency with MODIS, the comparison revealed systematic overestimation of productivity by CASA in both years. Mean positive biases were 123.62 gC $m^{-2}$ $yr^{-1}$ in 2020 and 73.67 gC $m^{-2}$ $yr^{-1}$ in 2025, indicating a reduction in discrepancy over time. Agreement metrics showed modest improvement in 2025, with RMSE decreasing from 204.00 to 191.41 gC $m^{-2}$ $yr^{-1}$ and MAE from 164.81 to 158.61 gC $m^{-2}$ $yr^{-1}$. However, pixel-level correspondence between the two products remained weak, as reflected by low coefficients of determination ($R^2$ = 0.03 in 2020; 0.04 in 2025).

Spatial agreement analysis further indicated that only ~46% of pixels in 2020 and ~45% in 2025 fell within ±20% of MODIS-derived NPP, confirming substantial spatial divergence between the datasets. This pattern is reinforced by the analysis of absolute scaling inconsistency (SI), which averaged 0.21 in 2020 and 0.20 in 2025, indicating approximately 20% relative deviation between CASA and MODIS estimates.

The spatial distribution of SI in Figure 1 reveals predominantly moderate agreement across the study area, interspersed with localized zones of high inconsistency (>0.40), particularly in central and southern regions. The persistence of these patterns across both years suggests that the observed discrepancies are systematic rather than random.

Collectively, these results indicate that while CASA and MODIS produce broadly comparable regional-scale productivity magnitudes, they differ markedly in their spatial representation of NPP, highlighting persistent scale-related inconsistencies between process-based model estimates and coarse-resolution satellite products.

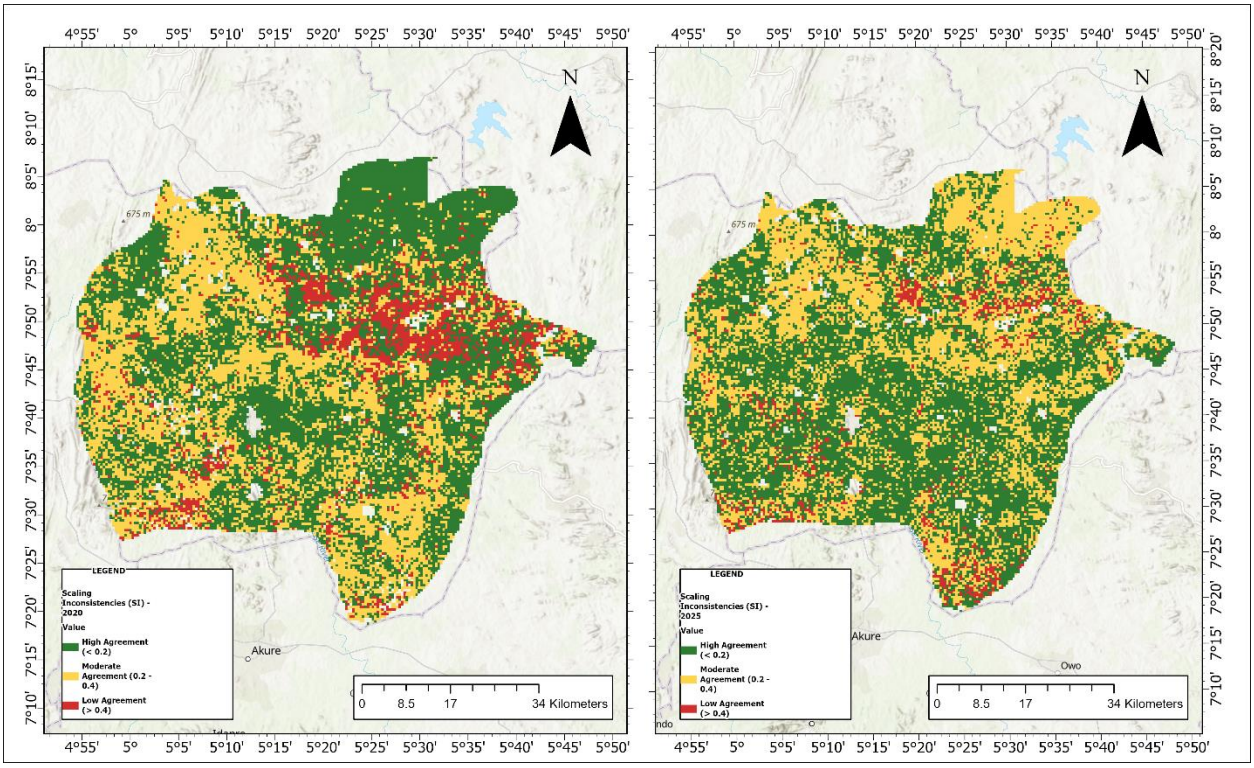


Figure 1: Scaling Inconsistency between CASA and MODIS NPP in 2020 and 2025

**Dimensional Inconsistency Between LULC and Canopy Height Using FAO-Aligned Thresholds (≥5 m and ≥10 m)**

The spatial distribution of LULC-derived forest and CHM-based forest thresholds shows clear differences across both years (Fig. 2). In this study, canopy height thresholds of ≥5 m and ≥10 m was applied to represent structural forest conditions, consistent with FAO definitions of woody vegetation and more developed forest canopy structure. In 2020, the LULC map (Fig. 2a) indicates a fragmented pattern of forest and non-forest areas across the study region. In contrast, the CHM ≥5 m layer (Fig. 2c) shows a largely continuous forest cover, with most pixels classified as forest. When the threshold is increased to ≥10 m (Fig. 2e), the extent of forest cover is substantially reduced, with more areas classified as non-forest.

A similar pattern is observed in 2025. The LULC-derived forest (Fig. 2b) remains spatially fragmented, while the CHM ≥5 m layer (Fig. 2d) again shows extensive forest coverage across the region. Under the ≥10 m threshold (Fig. 2f), forest cover decreases markedly, with a greater proportion of non-forest pixels compared to the ≥5 m condition.

Across both years, the CHM ≥5 m maps show consistently higher forest coverage than the LULC maps, while the CHM ≥10 m maps show reduced forest extent relative to both LULC and CHM ≥5 m outputs. The spatial patterns observed in 2020 and 2025 are broadly similar, with no major shifts in the overall distribution of forest and non-forest areas.

Comparison of forest extent between 2020 and 2025 shows broadly similar spatial distributions within each dataset type (Fig. 2). The LULC-derived forest maps for 2020 and 2025 (Fig. 2a–b) exhibit comparable patterns of fragmentation, with no pronounced shifts in the overall configuration of forest and non-forest areas. Similarly, the CHM ≥5 m layers (Fig. 2c–d) display consistently extensive forest coverage in both years, while the CHM ≥10 m layers (Fig. 2e–f) show reduced but spatially comparable distributions of taller canopy forest.

Despite this temporal consistency within datasets, differences between LULC and CHM-derived forest remain evident in both years. In 2020 and 2025, areas identified as forest in the CHM ≥5 m maps extend beyond those classified as forest in the LULC maps, while the CHM ≥10 m maps show a contraction of forest extent relative to LULC-derived forest. These relationships are consistent across both years, indicating stable patterns of correspondence and mismatch between spectral and structural representations of forest extent.

These spatial patterns are supported by structural validation metrics, which show lower agreement at the 5 m threshold, with F1-scores of approximately 0.58 in 2020 and 0.50 in 2025, alongside low recall values (<0.41). At the 10 m threshold, agreement improves, with F1-scores increasing to about 0.75 (2020) and 0.66 (2025). Across both thresholds, F1-scores decline slightly from 2020 to 2025, while overall accuracy remains relatively stable at approximately 0.76 under the 10 m threshold in both years.

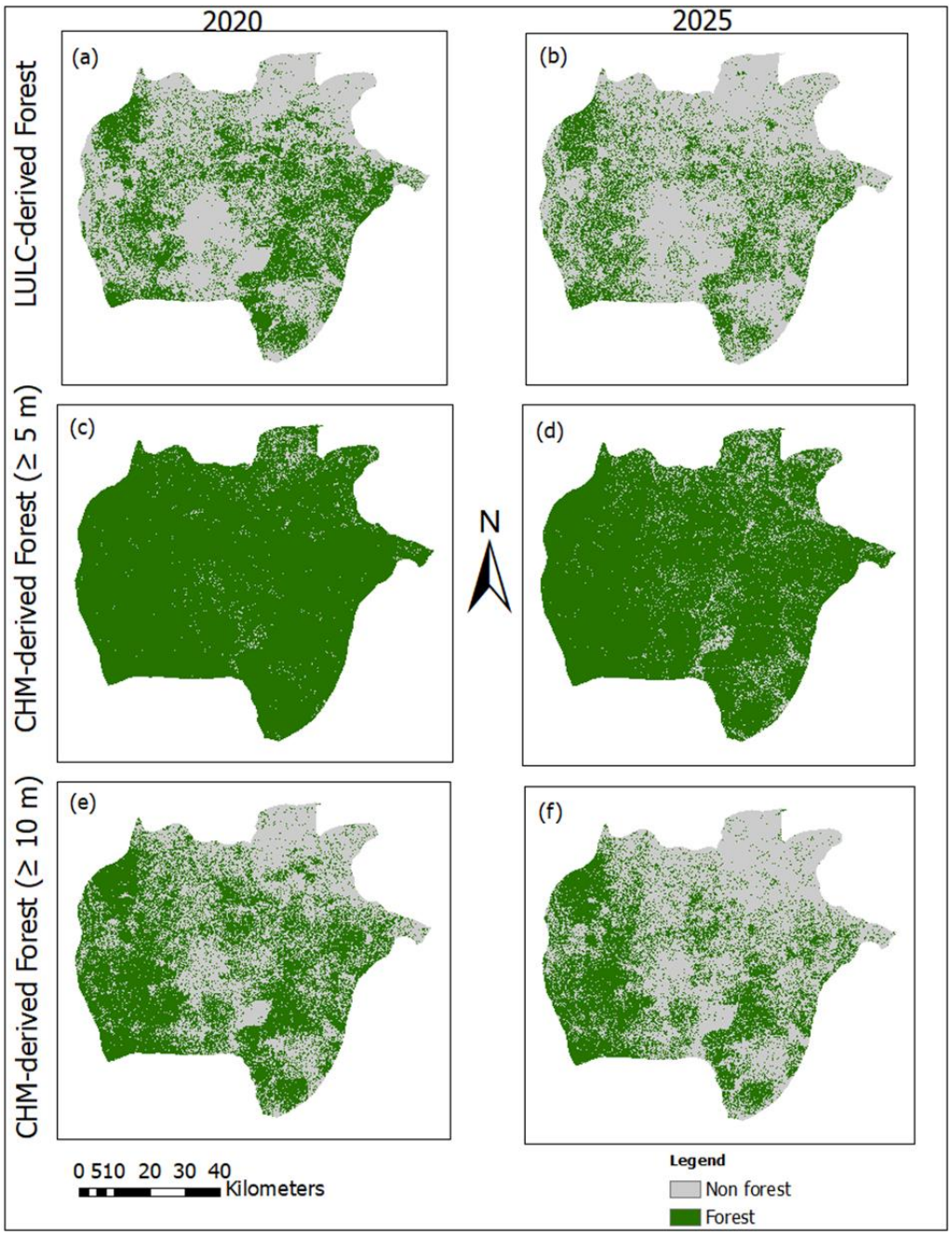


Figure 2. Comparison of LULC-derived and CHM-derived forest extent using FAO-aligned canopy height thresholds (≥5 m and ≥10 m) for 2020 and 2025.

**Variable Inconsistency Between Canopy Height and AGB**

The mean variable inconsistency (VI) was 0.18 (SD = 0.15), indicating generally low divergence between canopy height and aboveground biomass across the study area. The spatial distribution of VI in Figure 3 is dominated by low inconsistency values (VI < 0.20), reflecting a high level of agreement between CHM and AGB over most of the landscape. Moderate inconsistency (0.20–0.40) is widespread, while high inconsistency (VI > 0.40) occurs in localized clusters.

Low inconsistency values are predominantly associated with areas covered by forest and vegetation, where changes in canopy height and biomass appear broadly proportional. In contrast, higher inconsistency values are concentrated in impervious and open surfaces, where divergence between CHM and AGB is more pronounced.

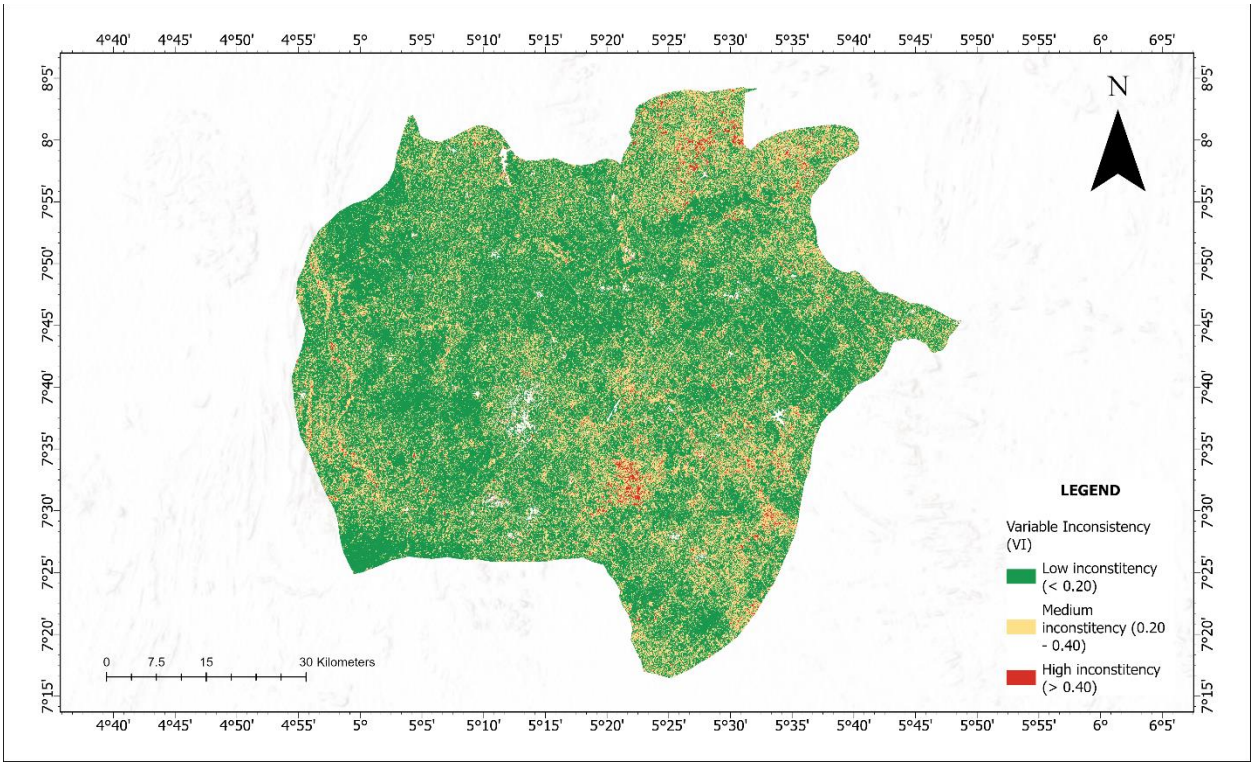


Figure: Figure 3: Spatial distribution of the Variable Inconsistency (VI) index

**Multi-Dimensional Inconsistency Index (MDII).**

The spatial distribution of the Multi-Dimensional Inconsistency Index (MDII) in Figure 4 indicates that moderate inconsistency (0.20–0.40) dominates across the study area, consistent with the mean MDII value of 0.26. High inconsistency (>0.40) occurs in localized clusters, particularly within transitional and fragmented landscapes, while low inconsistency (<0.20) is associated with relatively intact vegetation zones.

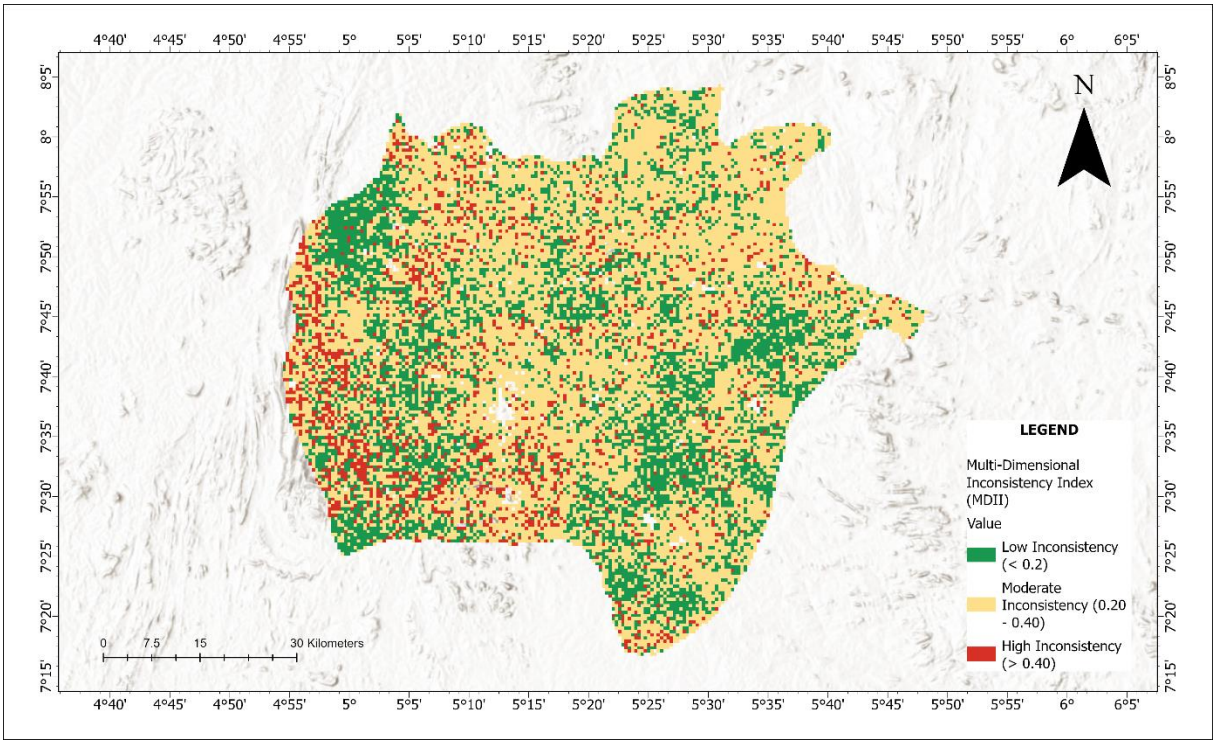


Figure 4: Spatial distribution of the Multi-Dimensional Inconsistency Index (MDII)

**DISCUSSION**

This study demonstrates that inconsistencies in remote sensing–based ecosystem assessment are systematic, hierarchical, and rooted in fundamentally different modes of environmental representation rather than random error or noise. The moderate overall inconsistency (MDII = 0.26) reveals a clear dominance structure among components: dimensional inconsistency (DI ≈ 0.41) is the primary driver, scale inconsistency (SI ≈ 0.20–0.21) is persistent but secondary, and variable inconsistency (VI ≈ 0.18) remains comparatively low. This hierarchy indicates that disagreement across datasets is governed more by how ecosystems are represented than by instability in ecological processes themselves.

These findings align with established evidence that remote sensing products are influenced by scale effects, classification uncertainty, and sensor-specific limitations (Woodcock & Strahler, 1987; Atkinson & Tate, 2000; Herold et al., 2008). However, rather than treating these issues independently, this study integrates them into a unified diagnostic framework. In doing so, the MDII reframes inconsistency from a limitation to a diagnostic property of multi-source Earth observation systems, enabling systematic interpretation of disagreement across spectral, structural, and carbon domains.

**Scale inconsistency: structural differences between modelled and satellite-derived productivity.**

The weak pixel-level agreement between CASA-derived and MODIS NPP ($R^2 \approx 0.03–0.04$) despite spatial aggregation demonstrates that harmonizing resolution alone cannot reconcile productivity datasets. Instead, scale inconsistency reflects deeper differences in model structure and ecological representation. CASA, as a light-use efficiency model, responds to local NDVI and climate inputs but relies on a constant LUE parameter, which simplifies spatial variability in vegetation physiology and stress. This leads to systematic overestimation of productivity in heterogeneous landscapes. In contrast, MODIS NPP applies biome-specific parameterisation and global calibration, producing smoother but more conservative estimates (Running et al., 2004; Zhao & Running, 2010).

This divergence is therefore epistemic rather than spatial: CASA emphasizes local sensitivity with simplified assumptions, whereas MODIS prioritizes global consistency at the expense of local variability. Similar discrepancies have been widely reported in productivity modelling studies, where outputs depend strongly on input datasets, parameterisation schemes, and scale (Turner et al., 2003; Pettorelli et al., 2014; Mbow et al., 2015; Bejide & Olaniran, 2026). The persistence of SI across both years confirms that this inconsistency is structurally embedded rather than incidental. Consequently, scale inconsistency should be interpreted as an inherent property of integrating process-based models with satellite-derived products, not an error that can be resolved through resampling.

**Dimensional inconsistency: evidence of spectral–structural divergence**

Dimensional inconsistency is the dominant source of disagreement, reflecting the fundamental mismatch between two-dimensional spectral classifications and three-dimensional canopy structure. The observed pattern, where CHM ≥5 m produces more extensive forest cover than LULC, while CHM ≥10 m produces less indicates that spectral products simultaneously under-detect structurally valid vegetation and overestimate mature forest extent. This is consistent with findings that land-cover classifications simplify heterogeneous landscapes into discrete categories, often masking internal structural variability (Herold et al., 2008).

The divergence arises from fundamental differences in sensor sensitivity. Optical remote sensing captures canopy greenness and cover but cannot directly measure vertical structure and is prone to saturation in dense vegetation (Hansen et al., 2013). In contrast, LiDAR provides direct measurements of canopy height, enabling detection of structural variation and degradation (Dubayah et al., 2020). The threshold-dependent results reinforce this interpretation: lower agreement at ≥5 m reflects the inability of spectral data to detect early-stage or low-stature woody vegetation, while improved agreement at ≥10 m indicates greater consistency for well-developed forest.

In degraded tropical landscapes, this mismatch is expected because processes such as selective logging, fuelwood extraction, and fragmentation reduce canopy height without necessarily altering spectral reflectance. As a result, forests may remain spectrally classified as intact while undergoing structural degradation. This confirms that the dominant uncertainty in forest monitoring is not classification accuracy per se, but the inability of two-dimensional spectral data to represent three-dimensional ecosystem structure. The results therefore provide strong empirical support for spectral–structural divergence as a central limitation in conventional remote sensing analyses (Gao et al., 2020; Mbow et al., 2015).

**Variable inconsistency: stability of structural–carbon relationships**

In contrast to the strong dimensional mismatch, variable inconsistency between canopy height and aboveground biomass is relatively low, indicating broadly coherent structural–carbon relationships within the study area. This suggests that, at the Ekiti scale, degradation is primarily expressed as

proportional structural thinning. However, this pattern is context-dependent. Evidence from broader Southwestern Nigeria analyses shows that structural–carbon decoupling can occur, with biomass losses exceeding corresponding changes in canopy height under more heterogeneous disturbance regimes (Bejide et al., 2026). The relatively low VI observed here therefore reflects a localized expression of degradation rather than a general absence of decoupling. Taken together, these findings indicate that structural–carbon relationships are scale- and context-dependent, with both proportional thinning and decoupling coexisting across landscapes.

**Integrated interpretation: what MDII reveals about ecosystem monitoring**

The MDII framework demonstrates that moderate overall inconsistency is driven primarily by dimensional mismatch rather than scale or variable effects. This is a critical insight because it identifies representation not ecological behaviour as the dominant source of uncertainty. The MDII therefore functions not as an accuracy metric, but as a diagnostic framework for identifying the dominant dimension of uncertainty in integrated remote sensing analyses.

This extends previous work on remote sensing uncertainty, which has largely focused on individual sources of error (Woodcock & Strahler, 1987; Atkinson & Tate, 2000; Herold et al., 2008). By integrating multiple dimensions of inconsistency, MDII enables a more comprehensive understanding of how different datasets interact. Importantly, it reveals that multi-source integration does not inherently improve ecosystem monitoring; instead, it may combine incompatible representations if underlying differences are not explicitly diagnosed. Spectral, structural, and model-based datasets capture different aspects of ecosystem condition, and their integration requires careful interpretation rather than assumption of agreement.

**Implications for forest monitoring and carbon assessment**

The dominance of dimensional inconsistency has direct implications for forest monitoring and carbon accounting. Spectral land-cover maps should not be interpreted as proxies for structural integrity, particularly in degraded or fragmented landscapes. Failure to account for this limitation may lead to systematic overestimation of intact forest area in operational monitoring systems, including REDD+ frameworks that rely heavily on spectral classifications.

The relative stability of structural–carbon relationships reinforce the importance of integrating LiDAR and SAR-derived structural data into monitoring systems. These datasets provide more

reliable indicators of forest condition and degradation, enabling detection of structural changes that are not visible in spectral data alone (Dubayah et al., 2020; Skole et al., 2021).

At the same time, persistent scale inconsistency highlights the need for cautious interpretation of productivity models. Without spatially adaptive parameterisation, models such as CASA may misrepresent local carbon dynamics, while global products such as MODIS may obscure fine-scale variability (Running et al., 2004; Pettorelli et al., 2014). This underscores the importance of combining model outputs with observational data to improve reliability.

**Limitations and future directions**

The study is subject to several limitations. GEDI data provide high-quality structural information but are constrained by discrete footprint sampling, which may not fully capture spatial heterogeneity (Dubayah et al., 2020). The use of a constant light-use efficiency parameter in CASA simplifies ecological processes and likely contributes to systematic bias. Additional uncertainties arise from temporal mismatches among datasets and potential errors in machine-learning-derived CHM and AGB estimates.

Future research should incorporate spatially variable model parameters, expand field validation, and integrate time-series structural datasets to better capture degradation dynamics. Extending the MDII framework to other ecological regions will also be essential for assessing its general applicability and identifying whether dimensional inconsistency remains the dominant source of disagreement across different landscapes.

**Conclusion of discussion**

Overall, this study shows that inconsistencies in remote sensing–based ecosystem assessment are systematic, hierarchical, and dimension-specific. The dominant source of disagreement is the mismatch between spectral land-cover representation and structural canopy reality, while structural–carbon relationships remain largely coherent and scale differences persist due to model assumptions. By explicitly diagnosing these inconsistencies, the MDII framework provides a pathway toward more defensible, interpretable, and policy-relevant ecosystem monitoring in data-rich but representation-limited remote sensing environments.

**Declaration of generative AI and AI-assisted technologies in the manuscript preparation process**

During the preparation of this work the author(s) used Google Gemini for language and grammatical accuracy correction. After using this tool/service, the author(s) reviewed and edited the content as needed and take(s) full responsibility for the content of the published article.

**FUNDING:** The author received no specific funding for this work.

REFERENCES

1. Atkinson, P. M., & Tate, N. J. (2000). Spatial scale problems and geostatistical solutions: A review. International Journal of Applied Earth Observation and Geoinformation, 2(3-4), 155–178.
2. Bejide O.D. & Olaniran H.D. (2026). Geospatial modelling of vegetation dynamics and carbon sequestration capacity in Ekiti State, Nigeria, using MODIS data and CASA models. *Turkisk Joournal of Remote Sensing*
3. Bejide O.D, Emiola K.D & Olaniran H.D. (2026). Structural–carbon decoupling and forest structural thinning in degrading forests of Southwestern Nigeria using GEDI LiDAR and multi-sensor data fusion. EarthAxiv. https://doi.org/10.31223/X5GB53
4. Costanza, R., De Groot, R., Sutton, P., Van der Ploeg, S., Anderson, S. J., Kubiszewski, I., ... & Turner, R. K. (2014). Changes in the global value of ecosystem services. *Global environmental change*, *26*, 152-158.
5. Dubayah, R., Blair, J. B., Goetz, S., Fatoyinbo, T., Hansen, M., Healey, S., Hofton, M., Luthcke, S., & Armston, J. (2020). The Global Ecosystem Dynamics Investigation: High-resolution laser ranging of the Earth's forests and topography. Science of Remote Sensing, 1, 100002. https://doi.org/10.1016/j.srs.2020.100002
6. Festus, I. A. (2012). Appraisal of the causes and consequences of human induced deforestation in Ekiti State, Nigeria. *Journal of Sustainable Development in Africa*, *14*(3), 37-52.
7. Gao, Y., Skutsch, M., Paneque-Gálvez, J., & Ghilardi, A. (2020). Remote sensing of forest degradation: A review. Environmental Research Letters, 15(10), 103001. https://doi.org/10.1088/1748-9326/abaad7
8. Hansen, M. C., Potapov, P. V., Moore, R., Hancher, M., Turubanova, S. A., Tyukavina, A., Thau, D., Stehman, S. V., Goetz, S. J., Loveland, T. R., Kommareddy, A., Egorov, A., Chini, L., Justice, C. O., & Townshend, J. R. G. (2013). High-resolution global maps of 21st-century forest cover change. Science, 342(6160), 850–853. https://doi.org/10.1126/science.1244693
9. Herold, M., Mayaux, P., Woodcock, C. E., Baccini, A., & Schmullius, C. (2008). Some challenges in global land cover mapping: An assessment of agreement and accuracy in existing 1 km datasets. Remote Sensing of Environment, 112(5), 2538–2556.
10. IPCC. (2021). Climate Change 2021: The Physical Science Basis. Cambridge University Press.

11. Mbow, C., Brandt, M., Ouedraogo, I., de Leeuw, J., & Marshall, M. (2015). What four decades of earth observation tell us about land degradation in the Sahel? Remote Sensing, 7(4), 4048–4067. https://doi.org/10.3390/rs70404048
12. Pettorelli, N., Laurance, W. F., O'Brien, T. G., Wegmann, M., Nagendra, H., & Turner, W. (2014). Satellite remote sensing for applied ecologists: Opportunities and challenges. Journal of Applied Ecology, 51(4), 839–848. https://doi.org/10.1111/1365-2664.12261
13. Running, S. W., Nemani, R. R., Heinsch, F. A., Zhao, M., Reeves, M., & Hashimoto, H. (2004). A continuous satellite-derived measure of global terrestrial primary production. BioScience, 54(6), 547–560.
14. Saatchi, S. S., Harris, N. L., Brown, S., Lefsky, M., Mitchard, E. T., Salas, W., ... & Morel, A. (2011). Benchmark map of forest carbon stocks in tropical regions across three continents. *Proceedings of the national academy of sciences*, *108*(24), 9899-9904.
15. Skole, D. L., Samek, J. H., Mbow, C., Chirwa, M., Ndalowa, D., Tumeo, T., Kachamba, D., Kamoto, J., Chioza, A., & Kamangadazi, F. (2021). Direct measurement of forest degradation rates in Malawi: Toward a national forest monitoring system to support REDD+. Forests, 12(4), 426. https://doi.org/10.3390/f12040426
16. Turner, W., Spector, S., Gardiner, N., Fladeland, M., Sterling, E., & Steininger, M. (2003). Remote sensing for biodiversity science and conservation. Trends in Ecology & Evolution, 18(6), 306–314.
17. Woodcock, C. E., & Strahler, A. H. (1987). The factor of scale in remote sensing. Remote Sensing of Environment, 21(3), 311–332.
18. Zhao, M., & Running, S. W. (2010). Drought-induced reduction in global terrestrial net primary production from 2000 through 2009. *science*, *329*(5994), 940-943.